Transient Cerebral Ischemia

Association of Apoptosis Induction with Hypoperfusion

Zinaida S. Vexler,*‡ Timothy P.L. Roberts,* Andrew W. Bollen,§ Nikita Derugin,* and Allen I. Arieff‡

**Department of Radiology, ‡Department of Medicine, and §Department of Pathology, University of California, San Francisco, San Francisco, California 94143*

Abstract

Apoptosis is thought to be important in the pathogenesis of cerebral ischemia. The mechanism of apoptosis induction remains unclear but several studies suggest that it is preferentially triggered by mild/moderate microcirculatory disturbances. We examined in cats whether induction of apoptosis after 2.5 h of unilateral middle cerebral artery occlusion plus 10 h of reperfusion is influenced by the degree of cerebral microcirculatory disturbance. Quantitative monitoring over time of the disturbances of cerebral microcirculation in ischemic brain areas and evaluation of cytotoxic edema associated with perfusion deficits was achieved by using two noninvasive magnetic resonance imaging techniques: (*a*) high-speed echo planar imaging combined with a bolus of magnetic susceptibility contrast agent; and (*b*) diffusion-weighted imaging. Apoptosis-positive cells were counted in anatomic areas with different severity of ischemic injury characterized by magnetic resonance imaging, triphenyltetrazolium chloride, and hemotoxylin and eosin staining. The number of apoptosis-positive cells was significantly higher in anatomic areas with severe perfusion deficits during occlusion and detectable histologic changes 10 h after reperfusion. In contrast, in areas where perfusion was reduced but maintained during occlusion there were no detectable histological changes and significantly fewer apoptosis-positive cells. A similar number of cells that undergo apoptosis were shown in regions with transient or prolonged subtotal perfusion deficits. These results suggest that the apoptotic process is induced in the ischemic core and contributes significantly in the degeneration of neurons associated with transient ischemia. (*J. Clin. Invest.*) 1997. 99: 1453–1459.) **Key words: apoptosis • middle cerebral artery occlusion • penumbra • cerebral perfusion • magnetic resonance imaging**

Introduction

Apoptosis is a physiologically essential mechanism of cell death that together with cell proliferation is responsible for the precise regulation of cell numbers for a variety of cell populations during normal development (1, 2). It also serves as a defense mechanism to remove unwanted and potentially dangerous cells (2). The inappropriate activation or inhibition of apoptosis, however, is now thought to cause or contribute to a variety of diseases, including cancer, stroke, brain trauma, epilepsy, and neurodegenerative diseases (2–4). It is becoming evident that cell exposure to the same pathologic stimuli such as free radicals, glutamate, and calcium can trigger both apoptosis and necrosis, two distinctly different types of cell death (2), and that the outcome of cell survival or evolution of either type of cell death can depend on the intensity of initial stimuli or a combination of type, intensity, and duration (5–7).

Focal permanent (3, 4, 8, 9) and transient (10) occlusion as well as transient global ischemia (11, 12) all can trigger apoptosis, and a variable susceptibility of different brain regions and timecourse of the induction of apoptosis has been noted (4, 10, 12). In a rat model of transient middle cerebral artery (MCA)[1] occlusion (10), apoptotic cells were reported on the penumbra edge of cortical infarction rather than in the core ischemic insult. Such a finding suggests that after transient MCA occlusion, microcirculatory disturbances that are mild to moderate can preferentially trigger apoptosis and contribute to the expansion of ischemic injury. These data raised questions as to the relationships between cerebral blood flow disturbances and susceptibility of cells to apoptosis, as well as the molecular mechanisms responsible for such a dependence. The thresholds of cerebral ischemia that are necessary for induction of functional, metabolic, and histologically detectable brain injury are known to differ substantially (13). Decrease of protein synthesis (14) and expression of early immediate genes are known to be among the most sensitive to subtle reductions of cerebral blood flow (13). It is unclear if a threshold for induction of apoptosis exists. If it does and diverse signals like oxidative stress (5, 15), glutamate release (5), calcium increase (16), and deprivation of growth factors (17) known to contribute to triggering apoptosis are important for such a threshold; then the lowering of threshold by pharmacological or genetic means might prove to be of clinical importance in the management of stroke.

To determine how induction of apoptosis caused by a transient cerebral occlusion relates to the degree of cerebral microcirculatory compromise, we evaluated the number of cells undergoing apoptosis in brain areas with different degrees of disturbances of cerebral microcirculation. By using magnetic resonance imaging (MRI), we quantitatively monitored over

Address correspondence to Zinaida S. Vexler, University of California, San Francisco, Department of Neurology, Box 0114, 521 Parnassus Ave., San Francisco, CA 94143. Phone: 415-502-5822; FAX: 415-502-5821; E-mail: zinaida@itsa.ucsf.edu

Received for publication 16 August 1996 and accepted in revised form 3 January 1997.

J. Clin. Invest.

0021-9738/97/03/1453/07 $2.00
Volume 99, Number 6, March 1997, 1453–1459

1. *Abbreviations used in this paper:* ADC, apparent diffusion coefficient; H&E, hemotoxylin and eosin; MCA, middle cerebral artery; MRI, magnetic resonance imaging; ROI, region of interest; TdT, terminal deoxynucleotidyl transferase; TTC, triphenyl-tetrazolium chloride; TUNEL, TdT-mediated deoxyuridine triphosphate-biotin nick end labeling.

time the disturbances of cerebral microcirculation in ischemic brain areas after transient MCA occlusion and evaluated cytotoxic edema associated with perfusion deficits. We demonstrated that although moderate cerebral hypoperfusion caused only a small number of cells to die by apoptosis, a significantly higher number of cells underwent apoptosis in regions that had transient or prolonged severe perfusion deficits.

Methods

Animal model and experimental protocol. The animal protocols used in this study were approved by the committee on animal research at the University of California (San Francisco, CA). Six young adult mixed-breed cats (2.5–3.5 kg) were anesthetized using short-acting barbiturate. Complete MCA occlusion was achieved by surrounding the MCA with nylon suture just proximal to the origin of the striate arteries, and then tightening the suture for 2.5–3 h. This was followed by a 10-h period of arterial reperfusion achieved by the untying and removal of the suture as previously described (18). Reperfusion upon removal of suture was documented in all animals, but variations in reperfusion profiles in different anatomic areas within the same brain were observed. Arterial blood pH, pO_2, pCO_2, and bicarbonate were measured hourly and respiratory rate and tidal volume adjustments were made when needed. Mean arterial blood pressure and heart rate were recorded every 5 min. During imaging, the cats were mechanically ventilated with 0.5–2% isoflurane in 30% O_2, 70% N_2O. Body temperature was maintained at 37°C. Contrast-enhanced and diffusion-sensitive imaging were performed 2 h after MCA occlusion and at various times after reperfusion. Brain tissue contralateral to occluded MCA vascular territory served as a control. At the conclusion of the MRI protocol, the animals were injected intracardially with triphenyl-tetrazolium chloride (TTC) as previously described (18, 19). The brains were removed for histopathological examination and immunostaining.

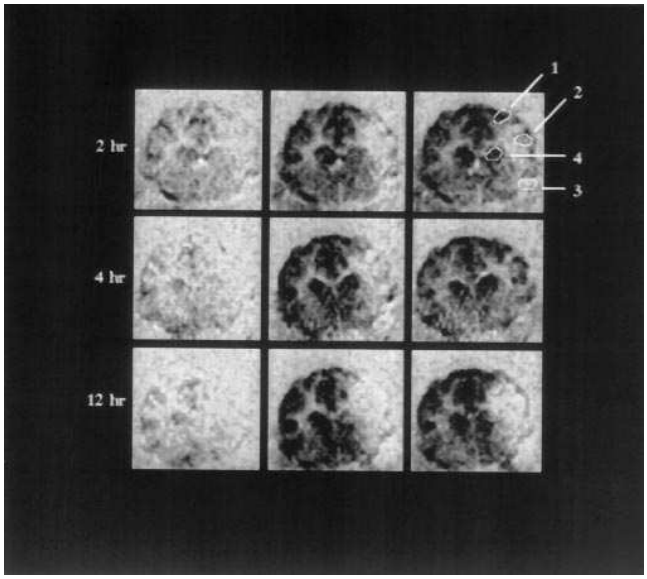

Figure 1. Contrast-enhanced MRI during unilateral MCA occlusion and reperfusion. Contrast transit is demonstrated 2 h (*top panel*), 4 h (*middle panel*), and 12 h (*bottom panel*) after MCA occlusion. The three images from the set of 16 images acquired at 2-s intervals correspond to the moments just before first arrival of the contrast agent, Sprodiamide Injection (0.25 mmol/kg, i.v. bolus), at: (*a*) the coronal imaging level (*left*); (*b*) during the peak of transit through (*middle*); and (*c*) the wash-out from the hemisphere contralateral to ischemia (*right*). Representative ROIs (*top right*) used for quantitative measurements in the hemisphere ipsilateral to MCA occlusion include an area in the medial parietal lobe (*1*), an area in the inferior parietal lobe (*2*), an area in the temporal lobe (*3*), and an area in the basal ganglia (*4*). ROIs of similar size and location were used in the hemisphere contralateral to MCA occlusion. Similar ROIs were assigned to the groups reflecting their perfusion status during reperfusion.

MRI. All imaging was performed using an Omega CSI (2T) system equipped with Acustar S-150 self-shielded gradients (±20 G/cm; Bruker Instruments, Fremont, CA). Perfusion-sensitive MRI was afforded by a combination of echo planar imaging and a bolus of intravascular magnetic susceptibility contrast agent, Sprodiamide Injection (0.25 mmol/kg, i.v.) (kindly provided by Nycomed-Salutar, Sunnyvale, CA) (Fig. 1). Images were acquired at 2-s intervals. The choice of contrast agent, dose of Sprodiamide Injection (0.25 mmol/kg) and frequency of use (every 1–2 h) were based on previous observations (18). Signal intensity in the control hemisphere was restored before each subsequent injection of contrast. The presence of the agent was detected as a transient signal loss in tissue surrounding the perfused microvasculature and converted in a ΔR_2^* format: $\Delta R_2^* = -\log [S(t)/S(0)]/TE$, where $S(t)$ and $S(0)$ are signal intensities at time t and 0, respectively. Since the contrast agent effect, characterized by ΔR_2^*, has been shown to be approximately proportional to its concentration (20, 21), estimates of rCBV can be obtained by temporal integration.

The ΔR_2^* values were then measured in several regions of interest (ROIs) in hemispheres ipsilateral and contralateral to the occlusion.

Diffusion-weighted imaging. Diffusion-weighted imaging is an MRI technique made sensitive to water diffusion over microscopic translational distances (22). Image intensity loss on diffusion-weighted imaging has been proposed (23, 24) to be associated with a bulk shift of water from the extracellular to the intracellular environment where interactions with macromolecules and organelle membranes inhibit water diffusion (19, 23, 24). Apparent diffusion coefficients (ADC) can be derived from a series of diffusion-weighted images with differing sensitivity to diffusion processes. Such ADC synthesis can be performed on a pixel-by-pixel basis to produce spatial maps. In diffusion-weighted images, Stejskal-Tanner pulsed gradients (8) were used with b values (diffusion-sensitivity factor) defined by: $S(b) \sim \exp(-bD)$, where b is the quantitative measure of the diffusion sensitivity of each MRI experiment and D represents the mean ADC of the protons in each image voxel.

ADC values were then measured in the same ROIs as those in which ΔR_2^* were measured.

TTC and hematoxylin and eosin histopathology. 60 ml of 2% TTC were injected intracardially at the end of the MRI experiment, 10 h after reperfusion. When either perfused intracardially or applied to individual brain sections (25), TTC appeared to accurately discriminate ischemic infarction from normally perfused tissue several hours after occlusion (26). The brains were removed, immediately fixed in 10% phosphate-buffered formalin and sectioned into 3–4-mm slices 24 h later. Discoloration of TTC-stained sections was analyzed with computer-assisted image analysis. Based on image analysis, severity of injury within ROIs, which closely resembled those chosen on MRI scans, was categorized as (*a*) severe (score 2) when a total absence of TTC staining was observed in ROIs, ipsilateral to the MCA occlusion; (*b*) moderate (score 1) when TTC staining was less intense than in the contralateral control hemisphere; and (*c*) normal (score 0) when no change in color was visible. The 3–4-mm coronal section from each brain that most closely matched a 4-mm plane on MRI scans was paraffin-embedded 72 h after the experiment. 5-μm coronal sections were cut. Adjacent sections were used for the detection of morphologic changes using hematoxylin and eosin (H&E) staining and the presence of apoptotic-positive cells.

In situ detection of apoptotic cells. The presence of apoptosis-positive cells was evaluated in situ by direct immunoperoxidase de-

Table I. Criteria for Constructing Subgroups on the Basis of Cerebral Microcirculation During MCA Occlusion and upon Reperfusion

Subgroup	Criteria		Anatomic region
	During occlusion	Upon reperfusion	
I ($n = 6$)	Severe hypoperfusion*	Severe hypoperfusion	Cortex
II ($n = 6$)	Severe hypoperfusion	Moderate hypoperfusion‡	Cortex
III ($n = 6$)	Moderate hypoperfusion	Remained perfused	Cortex
IV ($n = 4$)	Moderate hypoperfusion	Late decline of cerebral perfusion	Basal ganglia
V ($n = 2$)	Severe hypoperfusion	Moderate hypoperfusion	Basal ganglia

*Severe hypoperfusion is defined as the ratio $\Delta R_2^* < 20\%$ of the control value. ‡Tissue is described as moderately hypoperfused when the ratio ΔR_2^* was 40–60% of the control value.

tection of digoxigenin-labeled 3′-OH DNA strand breaks using the terminal deoxynucleotidyl transferase (TdT)-mediated deoxyuridine triphosphate–biotin nick end labeling (TUNEL) method (27). The procedure was as suggested by manufacture of a commercially available kit (ApopTag kit; Oncor Inc., Gaithersburg, MD). Protein digestion of deparaffinized tissue sections was achieved by treatment of the brain section with 20 μg/ml proteinase K (Sigma Chemical Co. St. Louis, MO) for 25–30 min at room temperature (rt). The adequacy of proteinase K digestion was established by a positive control, DNase I–treated section (10–15 ng/ml; 30 mM Trizma base, pH 7.2, 140 mM cacodylate, 4 mM $MgCl_2$, 0.1 mM dithiothreitol; 10 min at rt), as a parallel probe. For a slide serving as a negative control, procedures were identical to those used for the experiment with the only exception that TdT enzyme was omitted (distilled water substituted for enzyme). The model we used, that of unilateral MCA occlusion, enabled us to use anatomically matching areas localized contralateral to areas within the occluded MCA vascular territory as internal controls for each brain slide. Permount was used for mounting slides.

ROIs, quantitation of apoptosis-positive cells, and statistics. ROIs were selected on the earliest acquired contrast-enhanced images after MCA occlusion and after removal of suture, and ADC and ΔR_2^* measurements were accomplished. Fig. 1 (*top right*) demonstrates representative ROIs in the hemisphere ipsilateral to MCA occlusion. ROIs included three areas in the cortex, one in the medial parietal lobe (Fig. 1, *1*), another one in the inferior parietal lobe (Fig. 1, *2*) and one in temporal lobe (Fig. 1, *3*), and an area in basal ganglia (Fig. 1, *4*). Corresponding ROIs of similar size and location contralateral to the occlusion served as controls. Based on the profile of cerebral perfusion changes, five subgroups were constructed for evaluation of the relationships between the number of apoptosis-positive cells and the degree of hypoperfusion during occlusion and reperfusion. A 40–60% reduction in the ratio of ΔR_2^* in occluded/reperfused brain areas compared with the corresponding contralateral areas is referred to as "moderately hypoperfused," and "severe hypoperfusion" is defined by a ΔR_2^* ratio $< 20\%$. Criteria used for creating subgroups are listed in Table I.

For each ROI, a total of 15 to 20 100× fields of view were evaluated for the presence of positive cells, and 10 fields of view with the highest number of apoptosis-positive cells were selected, photographed, and then analyzed by two independent researchers. Stainable cells were identified morphologically with either methyl green or H&E and included neurons, glial, and endothelial cells. Endothelial cells, however, were excluded from the counting of the number of positive cells. Data were averaged and presented as mean±SEM for each individual ROI.

All data were subjected to statistical analysis using Bonferroni unpaired test using Statview IV (Abacus Concepts, Inc., Berkeley, CA) on a Macintosh computer. A two-tailed probability value of < 0.05 was considered significant.

Results

MRI findings. Blood pH , pCO_2, pO_2, and mean arterial blood pressure values were maintained within normal physiological range, and no significant changes in either parameters were observed during the entire experiment. Fig. 1 demonstrates an example of contrast-enhanced MRI acquired in both hemispheres of the same representative brain over time: during occlusion (*top panel*), 1.5 h (*middle panel*), and 10 h (*bottom panel*) after reperfusion. Each panel consists of three images: one precontrast image (*left column*), one image during the peak of first-pass transit of contrast agent through the hemisphere contralateral to occlusion (*middle column*), and one image during wash-out of this compound (*right column*). The ratio of peak ΔR_2^* measurements in ischemic compared with anatomically matched contralateral areas were limited to

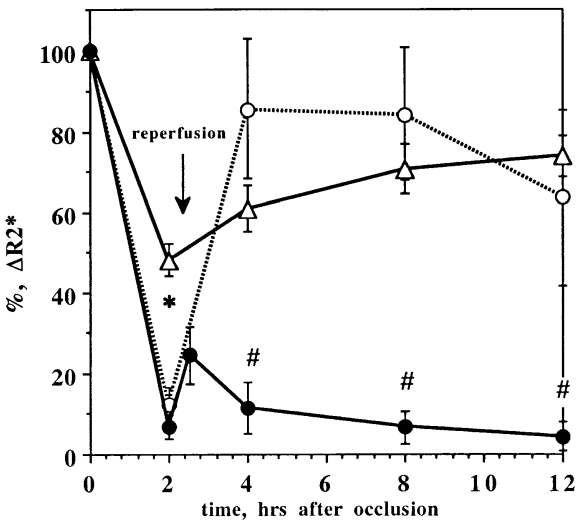

Figure 2. The ratio of peak ΔR_2^*, an indicator of cerebral microcirculation, in cerebral cortex of cats after transient MCA occlusion. Echo planar imaging was acquired before and during a bolus of magnetic susceptibility contrast agent, Sprodiamide Injection (0.25 mmol/kg), at indicated times during a 2.5-h occlusion period and upon reperfusion. Shown are subgroup I (-●-); subgroup II (-○-), and subgroup III (-△-). Mean±SEM ($n = 6$) are presented. *$P < 0.05$, subgroups I and II vs. subgroup III; #$P < 0.05$, subgroup I vs. subgroups II and III at corresponding time points.

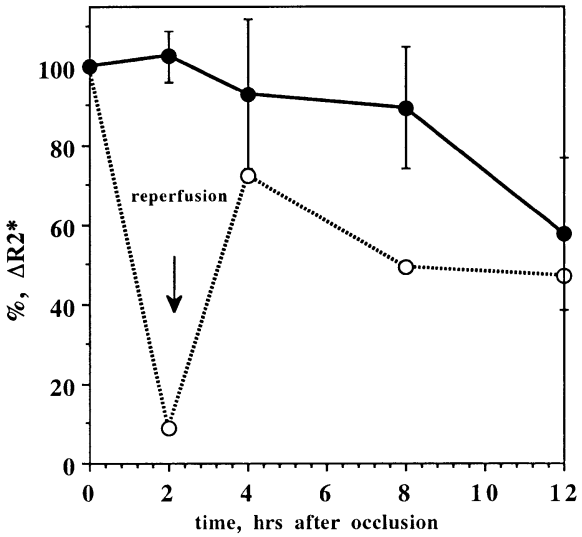

Figure 3. Time course of the ratio of peak ΔR_2* in basal ganglia of cats after transient MCA occlusion. Shown are subgroup IV (-●-) and subgroup V (-○-). Mean±SEM are presented. Experimental protocol is the same as in Fig. 2.

ROIs indicated on Fig. 1 (*top right*) with numbers 1–4. In this particular example, during MCA occlusion severe hypoperfusion (see Methods for definitions) was observed in ROIs 2 and 3, moderate hypoperfusion was seen in ROI 1, and mild hypoperfusion was seen in ROI 4. 1.5 h after reperfusion, moderate (ROIs *1* and *2*), severe (ROI *3*) hypoperfusion, and normal perfusion (ROI *4*) were observed (*middle panel*). A delayed decline of cerebral perfusion (*bottom panel*, ROIs *1–3*) and expansion of injured brain areas were observed at later time points. The time course of changes for the ratio of peak ΔR_2* effects for each individual ROI was analyzed in all brains, and subgroups I–III for cortical regions and subgroups IV and V for basal ganglia (Table I) were constructed based on a similarity of the ΔR_2* ratio profiles vs. time in chosen ROIs. Profiles of cerebral microcirculatory disturbances in subgroups I–V are demonstrated on Figs. 2 and 3. For example, on Fig. 1, ROI 1 is a constituent of subgroup III, ROI 2 is a part of subgroup II, ROI 3 is a part of subgroup I, and ROI 4 belongs to subgroup IV.

A statistically significant difference between peak ΔR_2* effects at various time points during occlusion ($P < 0.05$; subgroup III vs. subgroups I and II) and after reperfusion ($P < 0.05$; subgroup I vs. subgroups II and III) justified such a split (Fig. 2). The ratio of peak ΔR_2* between subgroups I and II was not statistically different during MCA occlusion, but was statistically significant ($P < 0.05$) at various times after reperfusion (Fig. 2). Although statistical comparisons between the ratio of peak ΔR_2* cannot be made between subgroups IV and V ($n = 2$ for subgroup V), Fig. 3 clearly demonstrates the different profile of the ratio of peak ΔR_2* changes during MCA occlusion.

In the areas contralateral to MCA occlusion, mean values of the ADC were $77\pm3 \times 10^{-7}$ cm^2/s for cortex and $80\pm3 \times 10^{-7}$ cm^2/s for basal ganglia and are in agreement with previous studies (23, 24, 28). Ipsilateral to the occlusion, significantly lower ADC values ($P < 0.05$), $48\pm3 \times 10^{-7}$ cm^2/s for subgroup I and $54\pm6 \times 10^{-7}$ cm^2/s for subgroup II, were determined during occlusion. These subgroups were characterized by severe perfusion deficits. After reperfusion, ADC values in subgroups I and II remained significantly lower ($P < 0.05$) compared with ADC values in normal hemisphere (not shown). In subgroup III, ADC values were $70\pm4 \times 10^{-7}$ cm^2/s and were not significantly different ($P > 0.05$) compared with normal cortex and remained unchanged during a reperfusion period. The same tendency towards decrease of the ADC values in areas of perfusion deficits was detected in basal ganglia; the ADC values were 64×10^{-7} cm^2/s for subgroup V compared with $70\pm6 \times 10^{-7}$ cm^2/s for subgroup IV and to $80\pm3 \times 10^{-7}$ cm^2/s in normal tissue.

TTC and H&E histology. Perfusion with TTC was used to demarcate ischemic areas. The entire hemisphere contralateral to the occlusion and part of the hemisphere ipsilateral to the occlusion appeared normal. Discoloration of the MCA vascular territory ipsilateral to the occlusion varied in different anatomic areas within the same brain and between different animals. A representative example of a TTC-stained brain shown in Fig. 4 *A* demonstrates severe injury in the basal ganglia, and middle parietal and temporal lobes, but no injury in the inferior parietal lobe. Two boundaries, one in the right cortex and the other in basal ganglia, show areas that are used for higher magnification pictures in Fig. 4, *B–G.* Severe hypoperfusion of cortical tissue, subgroup I (Fig. 4 *A*, *boundary*) was associated with perineuronal vacuolation and alterations of cell shape, as was evident from H&E staining (Fig. 4 *B*). Some neurons featured eosinophilic cytoplasm (ischemic neuron). In subgroup II, abnormal looking neurons coincided with neurons with no obvious signs of injury, indicating a lesser extent of injury (not shown). No morphologic features of injury were detected in tissue contralateral to occlusion (Fig. 4 *C*), as well as in tissue moderately hypoperfused through the entire study (subgroups III and IV, not shown).

The severity scores of ischemia-induced brain damage were as follows: (*a*) 2.0 for subgroup I; (*b*) 1.7 for subgroup II; (*c*) 0.2 for subgroup III; (*d*) 0.8 for subgroup IV; and (*e*) 2.0 for subgroup V. Thus, an early decline of cerebral microcirculation after reperfusion (subgroup I) resulted in severe injury. Even a prolonged period of recirculation of cortical tissue that was severely hypoperfused during the occlusion period (subgroup II) did not preserve tissue from relatively severe injury, as delineated by two measures, ADC values and TTC severity scores.

Apoptosis-positive cells. No stainable cells were found in the entire brain sections when water was substituted for TdT

Table II. Number of Apoptosis-positive Cells in Brain Tissue With Different Profiles of Microcirculatory Disturbance After Transient MCA Occlusion in the Cat*

ROI subgroup	Left	Right
I	0.4±0.3‡	20.1±2.6
II	0.5±0.3‡	23.5±4.1
III	0.0±0.0	2.3±1.4§‖
IV	0.0±0.0	6.0±1.7
V	0.0±0.0‡	22.0±5.0

*Presented are mean±SEM from sums of 10 chosen fields within each individual ROI. ‡Right vs. matching left, $P < 0.05$. §Right cortex vs. cortex from subgroup I, $P < 0.05$. ‖Right cortex vs. cortex from subgroup II, $P < 0.05$.

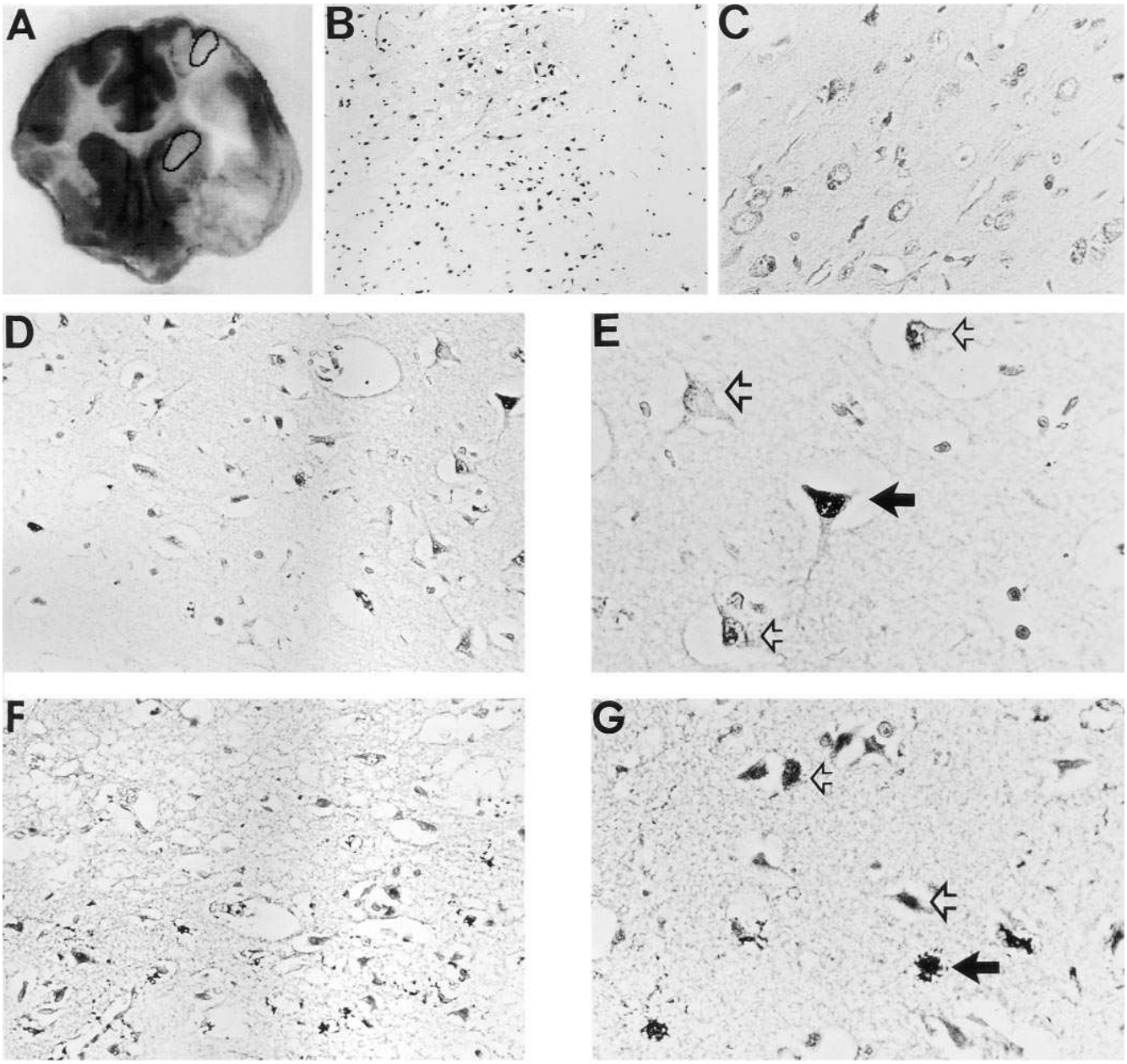

Figure 4. TTC, H&E, and immunostaining for apoptosis in a coronal section of representative severely injured cat brain. (*A*) TTC staining and ROIs selected for presenting of higher magnification pictures (*B–G*). (*B*) H&E staining (40×) demonstrates the presence of perineuronal vacuolation in parietal lobe ipsilateral to MCA occlusion. (*C–G*) ApopTag staining (250×) in contralateral (*C*) (200×) and ipsilateral (*D*) to ischemia parietal lobe, and in ipsilateral basal ganglia (*F*) (200×). High magnification (400×) of ApopTag staining (*E* and *G*) ipsilateral to occlusion shows apoptosis-positive (*solid arrows*), unstained (*hollow arrows*), and faintly stained (*small hollow arrows*) neurons in cortex (*E*) and basal ganglia (*G*).

(negative controls) in TUNEL assay. In the hemisphere contralateral to ischemia, only a few stainable cells per section were found (Table II). In subgroups I and II, which were ipsilateral to the occlusion, nonstained (Fig. 4, *E* and *G*, *hollow arrow*), intensely stained (Fig. 4, *E* and *G*, *solid arrows*), and bleary stained cells (Fig. 4 *E* and *G*, *small hollow arrows*) were all observed only in the vascular MCA territory. Faint staining appeared to be more diffuse compared with that in intensely stainable cells. Only clearly stained cells were considered to be apoptosis positive and were counted. Ipsilateral to the occlusion, apoptosis-positive neurons were seen more often than glial cells, but we did not specify a cell type because in some cases the plane sectioning did not enable accurate identification of cell type.

Groups of positive cells, as well as single cells dispersed throughout the ROIs, tested ipsilateral to occlusion in subgroups I, II, and V. The light microscopic appearance of apoptotic neurons was diverse. Although the shape of some positive cells was relatively normal, the majority of stainable cells were shrunken (Fig. 4, *E* and *G*, *arrows*). Multiple dark masses char-

acteristic for late stage of internucleosomal degradation (Fig. 4 *G*, *arrow*) were evident in some, but not all, cells. Ipsilateral to the occlusion, the number of apoptotic cells was significantly higher for subgroups I and II compared with corresponding control values (Table II). At the same time, the number of apoptotic cells was not significantly different ($P > 0.05$) between these subgroups, which were characterized by similar profile of cerebral microcirculation changes during the period of transient MCA occlusion, but by a distinctly different microcirculatory profile after reperfusion (Fig. 2). In moderately perfused cortical areas, the number of apoptotic cells was not significantly different from that in normal tissue (Table II), both in cortex and basal ganglia.

Discussion

This study demonstrates that the number of apoptotic cells is related to the degree of perfusion deficits during transient cerebral ischemia. This was found both in the cortex and basal ganglia. A significantly higher number of apoptotic cells was observed in anatomic areas associated with severe perfusion deficits during the occlusion period as compared with the number of apoptotic cells in brain areas in which perfusion was reduced but still present. In our previous study (18), such cortical areas with perfusion deficits have been demonstrated to develop infarction.

Quantitation of cerebral microcirculation and cytotoxic edema in various brain areas after transient MCA occlusion enabled us to couple induction of apoptosis to the degree of perfusion disturbances. We characterized disturbances of cerebral microcirculation by using the time integral of the ΔR_2* curve. The peak of ΔR_2* effect is thought to be proportional to the regional cerebral blood volume (29) and has been proven (18, 23, 24) to accurately demarcate the progression of ischemia. Cytotoxic edema associated with severe disturbances of the cerebral microcirculation was characterized by the ADC, which is thought to be associated with a shift of water from the extracellular to the intracellular environment early after stroke (23, 24, 30). Moderate hypoperfusion after cerebral ischemia did not result in a decrease of the ADC, in agreement with previous findings (19, 28, 31, 32). Severe perfusion deficits within the MCA vascular territory, however, resulted in a significant decrease of the ADC shortly after occlusion, indicating metabolic disturbances in such areas (32, 33). There was a decline of cerebral perfusion in the cerebral cortex after MCA occlusion but, in four animals, perfusion of the basal ganglia was maintained (Fig. 3), suggesting variation of collaterals to the basal ganglia in some cats.

We used a TUNEL method to measure the number of cells with initiated apoptosis. In earlier reports, investigators have used a combination of two to three methods to detect and ascertain the presence of apoptotic type of cell death in brain tissue while using various in vivo models. A combination of immunocytochemical methods such as TUNEL or flow cytometry with biochemical methods such as agarose gel electrophoresis (3, 10, 11), activation of Ca^{2+}-dependent DNA endonuclease (4, 34), or electron microscopy (35) generally showed good correlation between such independent measures. A TUNEL method was demonstrated to offer high sensitivity, showed good correlation with the presence of the nucleosome laddering pattern on agarose gel electrophoresis (characteristic of apoptosis), and provided an advantage of anatomic preciseness. Concerns that because of the sensitivity to the presence of free OH′ groups (this method can stain not only apoptotic cells but also necrotic cells) were addressed in several publications (10, 34, 36). Although faint staining of a number of cells has been attributed to the presence of marginally stainable concentrations of 5′-OH′ groups in necrotic cells, TUNEL method was considered sufficient to identify apoptotic cells when used with hematoxylin counterstaining and morphologic criteria (36). In this study, caution was taken in counting only intensely but not faintly stained cells and describing morphological appearance of apoptosis-positive cells.

Apoptosis was induced in tissue that experienced severe perfusion deficits and resulted in severe injury scores, rather than in penumbra, a moderately hypoperfused tissue peripheral to the ischemic core. Although different definitions of penumbra were given based on various functional and metabolic parameters (13), the two common features of penumbra include partial disruption of cerebral blood flow and reversibility of the ischemic injury. As a tissue at 'risk,' such areas are thought to be potentially resuscitatable and are the targets for therapeutic intervention. Our data demonstrate that moderate reductions of cerebral perfusion alone did not lead to a significant induction of apoptosis in cat brain during the duration of reperfusion that we studied. However, selective cell populations may be preferentially vulnerable to more subtle reductions of cerebral microcirculation that otherwise do not disturb metabolic and functional integrity. It may be that there is an "ischemic threshold" of hypoperfusion that activates apoptosis. Recent data have demonstrated that at later time points after mild transient cerebral ischemia in the rat, a substantial number of neurons from the periinfarct area undergo apoptosis (36, 37), and that more severe ischemic insult resulted in a higher number of apoptotic neurons. Species differences may in part account for differences between the observations reported here and previously published data (10). The rat is a species known to have lower brain collateral blood supply and less extended penumbra areas (13) than is found in cats.

The number of apoptotic cells was not significantly different ($P > 0.05$) in tissues with similar degrees of microcirculatory disturbances during the period of occlusion, but with distinctly different microcirculatory profile after reperfusion (Figs. 2 and 3). There was induction of apoptosis in areas with perfusion deficits during occlusion, regardless of the microcirculatory profile after reperfusion, suggesting that occlusion may play an important role in predisposing cells to apoptosis hours after reperfusion. Recent data using permanent occlusion (3) and as early as 0.5 h after transient focal ischemia (10) also supports the notion that severe perfusion deficits can initiate apoptotic process. Reperfusion is thought to be important in turning on programmed cell death mechanism (15, 16) as presumed primarily by the generation of free radicals associated with recirculation and reoxygenation of developing lesions. Suppression of free radicals production by the bcl-2 gene both in vitro (38) and in vivo (9) appeared to prevent apoptotic cell death. Reduction of infarct size and diminished apoptosis in rats focally overexpressing bcl-2 gene (9) and lower susceptibility of neurons expressing bcl-2 gene to ischemic insult (7) also points towards the importance of this mechanism for induction of apoptosis.

Our data as well as findings by others (10) indicate that apoptosis precedes morphological indications of ischemic cell damage associated with necrosis. At the same time, data by

Linnik et al. (9) and findings of the current study demonstrate that neurons committed to die by apoptosis and by necrosis localize in the core of ischemic injury. The meaning of this finding for the pathophysiology of stroke is yet to be determined. Concomitant presence of both necrotic and apoptotic cells may just reflect the fact that two pathophysiological pathways for cell death exist independently of each other, or, alternatively, indicate the existence of different thresholds for cell commitment to irreversible changes along alternative pathophysiological processes. As an example, the increased intensity of the same stimuli appeared to predispose neurons to necrotic rather than to an apoptotic death (6).

We demonstrated that apoptosis is triggered in brain regions that experienced severe perfusion deficits during occlusion rather than in areas with reduced but maintained perfusion. These results suggest that the apoptotic process contributes substantially to the degeneration of neurons associated with transient ischemia. Further studies of the role of the disturbances of the cerebral microcirculation to the process by which irreversible commitment of cells to apoptosis develops may lead to an understanding of the contribution of this process to the pathogenesis of stroke.

Acknowledgments

The authors thank Dr. I. Klimanskya for useful discussions regarding the sensitivity of the apoptosis assay.

This work was supported by National Institutes of Health grant AG-08575 from the National Institute on Aging (A.I. Arieff), by RREF grant, University of California, San Fransisco (Z.S. Vexler), and the Research Service of the Veterans Affairs Medical Center, San Francisco.

References

1. Raff, M.C., B.A. Barres, J.F. Burne, H.S. Cole, Y. Ishizaki, and M.D. Jacobson. 1993. Programmed cell death and the control of cell survival: lessons from the nervous system. *Science (Wash. DC)*. 262:695–700.

2. Steller, H. 1995. Mechanisms and genes of cellular suicide. *Science (Wash. DC)*. 267:1445–1449.

3. Linnik, M., R. Zobrist, and M. Hatfield. 1993. Evidence supporting a role for programmed cell death in focal cerebral ischemia in rats. *Stroke.* 24:2002–2008.

4. Tominaga, T., S. Kure, K. Narisawa, and T. Yoshimoto. 1993. Endonuclease activation following ischemic injury in the rat brain. *Brain Res.* 608:21–26.

5. Coyle, J.T., and P. Puttfarcken. 1993. Oxidative stress, glutamate, and neurodegenerative disorders. *Science (Wash. DC)*. 262:689–695.

6. Bonfoco, E., D. Krainc, M. Ankarcrona, P. Nicotera, and S. Lipton. 1995. Apoptosis and necrosis: two distinct events induced, respectively, by mild and intense insults with *N*-methyl-D-aspartate or nitric oxide/superoxide in cortical cell cultures. *Proc. Natl. Acad. Sci. USA.* 92:7162–7166.

7. Chen, J., S. Graham, P. Chan, J. Lan, R. Zhou, and R. Simon. 1995. Bcl-2 is expressed in neurons that survive focal ischemia in the rat. *Neuroreport.* 6: 394–398.

8. Stejskal, E., and J. Tanner. 1965. spin diffusion measurements: spin-echoes in the presence of a time-dependent field gradient. *J. Chem. Phys.* 42:288–292.

9. Linnik, M., P. Zahos, M. Geschwind, and H. Federoff. 1995. Expression of bcl-2 from a defective herpes simplex virus-1 vector limits neuronal death in focal cerebral ischemia. *Stroke.* 26:1670–1674.

10. Li, Y., M. Chopp, N. Jiang, F. Yao, and C. Zaloga. 1995. Temporal profile of in situ DNA fragmentation after transient middle cerebral artery occlusion in the rat. *J. Cereb. Blood Flow Metab.* 15:389–397.

11. Heron, A., H. Pollard, F. Dessi, J. Moreau, F. Labennes, Y. Ben-Ari, and C. Charriaut-Marlangue. 1993. Regional variability in DNA fragmentation after global ischemia evidenced by combined histological and gel electrophoresis observation in the rat brain. *J. Neurochem.* 61:1973–1976.

12. MacManus, J.P., A.M. Buchan, I.E. Hill, I. Rasqueinh, and E. Preston. 1993. Global ischemia can cause DNA fragmentation indicative of apoptosis in rat brain. *Neurosci. Lett.* 164:89–92.

13. Hossman, K. 1994. Viability thresholds and the penumbra of focal ischemia. *Ann. Neurol.* 36:557–565.

14. Mies, G., K. Kohno, and K. Hossman. 1993. MK-801, a glutamate antagonist, lowers flow threshold for inhibition of protein synthesis after middle cerebral artery occlusion of rat. *Neurosci. Lett.* 155:65–68.

15. Thompson, C. 1995. Apoptosis in the pathogenesis and treatment of disease. *Science (Wash. DC)*. 267:1456–1462.

16. Kiyota, Y., K. Pahlmark, H. Memezawa, M. Smith, and B. Siesjo. 1993. Free radicals and brain damage due to transient middle cerebral artery occlusion: the effect of dimethylthiourea. *Exp. Brain Res.* 95:388–396.

17. Yao, R., and G. Cooper. 1995. Requirement for phosphatidylinositol-3 kinase in the prevention of apoptosis by nerve growth factor. *Science (Wash. DC)*. 267:2003–2006.

18. Kucharczyk, J., Z. Vexler, T.P. Roberts, H. Asgari, N. Derugin, and M. Moseley. 1993. Echo planar perfusion-sensitive imaging of acute cerebral ischemia. *Radiology.* 188:711–717.

19. Roberts, T., Z. Vexler, N. Derugin, M. Moseley, and J. Kucharczyk. 1993. High-speed MR imaging of ischemic brain injury following partial stenosis of the middle cerebral artery. *J. Cereb. Blood Flow Metab.* 13:940–946.

20. Belliveau, J.W., B.R. Rosen, H.L. Kantor, R.R. Rzedzian, D.N. Kennedy, R.C. McKinstry, J.M. Vevea, M.S. Cohen, I.L. Pykett, and T.J. Brady. 1990. Functional cerebral imaging by susceptibility-contrast NMR. *Magn. Resn. Med.* 14:538–546.

21. Villinger, A., B.R. Rosen, J.W. Belliveau, J.L. Ackerman, R.B. Lauffer, R.B. Buxton, Y.S. Chao, V.J. Wedeen, and T.J. Brady. 1988. Dynamic imaging with lanthanide chelates in normal brain: contrast due to magnetic susceptibility effects. *Magn. Resn. Med.* 6:164–174.

22. LeBihan, D. 1990. Magnetic resonance imaging of perfusion. *Magn. Reson. Med.* 14:283–292.

23. Moseley, M.E., J. Kucharczyk, J. Mintorovitch, Y. Cohen, J. Kurhanewicz, N. Derugin, H. Asgari, and D. Norman. 1990. Diffusion-weighted MR imaging of acute stroke: correlation with T2-weighted and magnetic susceptibility-enhanced MR imaging in cats. *AJNR.* 11:423–429.

24. Moseley, M.E., Y. Cohen, J. Mintorovitch, L. Chileutt, H. Shimizu, J. Kucharczyk, M.F. Wendland, and P.R. Weinstein. 1990. Early detection of regional cerebral ischemia in cats: comparison of diffusion and T2-weighted MRI and spectroscopy. *Magn. Resn. Med.* 14:330–346.

25. Dettmers, C., A. Hartmann, T. Rommel, S. Kramer, S. Pappata, A. Young, S. Hartmann, S. Zierz, E. MacKenzie, and J. Baron. 1994. Immersion and perfusion staining with 2,3,5-triphenyltetrazolium chloride (TTC) compared to mitochondrial enzymes 6 hours after MCA-occlusion in primates. *Neurol. Res.* 16:205–208.

26. Bederson, J., L. Pitts, S. Germano, M. Nishimura, R. Davis, and H. Bartkowski. 1986. Evaluation of 2,3,5-triphenyltetrazolium chloride as a stain for detection and quantification of experimental cerebral infarction in rats. *Stroke.* 17:1304–1308.

27. Gavrieli, Y., Y. Sherman, and S. Ben-Sasson. 1992. Identification of programmed cell death in situ via specific labeling of nuclear DNA fragmentation. *J. Cell Biol.* 119:493–501.

28. van Bruggen, N., B. Cullen, M. King, M. Doran, S. Williams, D. Gadian, and J. Cremer. 1992. T2- and diffusion-weighted magnetic resonance imaging of a focal ischemic lesion in rat brain. *Stroke.* 23:576–582.

29. Rosen, B., J. Belliveau, and D. Chien. 1989. Perfusion imaging by nuclear magnetic resonance. *Magn. Resn. Q.* 5:263–281.

30. Benveniste, H., L.W. Hedlund, and G.A. Johnson. 1992. Mechanism of detection of acute cerebral ischemia in rats by diffusion-weighted magnetic resonance microscopy. *Stroke.* 23:746–754.

31. Roberts, T., Z. Vexler, V. Vexler, N. Derugin, and J. Kucharczyk. 1996. Sensitivity of high-speed 'perfusion' MRI to mild cerebral ischemia. *Eur. Radiology.* 6:645–649.

32. Vexler, Z., J. Ayus, T. Roberts, J. Kucharczyk, C. Fraser, and A. Arieff. 1994. Ischemic or hypoxic hypoxia exacerbates brain injury associated with metabolic encephalopathy in laboratory animals. *J. Clin. Invest.* 93:256–264.

33. Vexler, Z.S., T.P.L. Roberts, N. Derugin, E. Kozniewska, A.I. Arieff, and J. Kucharczyk. 1994. Mechanisms of brain injury associated with partial and complete occlusion of the MCA in cat. *Acta Neurochir. Suppl.* 60:211–215.

34. Charriaut-Marlangue, C., I. Margail, M. Plotkine, and Y. Ben-Ari. 1995. Early endonuclease activation following reversible focal ischemia in the rat brain. *J. Cereb. Blood Flow Metab.* 15:385–388.

35. Portera-Cailliau, C., J. Hedreen, D. Price, and V. Koliatsos. 1995. Evidence for apoptotic cell death in Huntington disease and excitotoxic animal models. *J. Neurosci.* 15:3775–3787.

36. Li, Y., M. Chopp, N. Jiang, Z. Zhang, and C. Zaloga. 1995. Induction of DNA fragmentation after 10 or 120 minutes of focal cerebral ischemia in rats. *Stroke.* 26:1252–1258.

37. Du, C., R. Hu, C. Csernansky, C. Hsu, and D. Choi. 1996. Very delayed infarction after mild focal cerebral ischemia: a role for apoptosis? *J. Cereb. Blood Flow Metab.* 16:195–201.

38. Hockenbery. 1993. Bcl-2 functions in an antioxidant pathway to prevent apoptosis. *Cell.* 75:241–251.